

High order fast sweeping methods for Eikonal equations

Yong-Tao Zhang, UC Irvine; Hong-Kai Zhao, UC Irvine; Jianliang Qian*, UCLA

Summary

We construct high order fast sweeping numerical methods for computing viscosity solutions of static eikonal equations on rectangular grids which yield first-arrival traveltimes. These methods combine high order weighted essentially non-oscillatory (WENO) approximation to derivatives, monotone numerical Hamiltonians and Gauss Seidel iterations with alternating-direction sweepings. Based on well-developed first order sweeping methods, we design a novel approach to incorporate high order approximations to derivatives into numerical Hamiltonians such that the resulting numerical schemes are formally high order accurate and inherit the fast convergence from the alternating sweeping strategy. Extensive numerical examples verify efficiency, convergence and high order accuracy of the new methods.

Introduction

Traveltime computation is an essential ingredient for Kirchhoff migration based high resolution seismic imaging. The first arrival traveltime in isotropic media corresponds to the viscosity solution of the standard isotropic Eikonal equation

$$|\nabla\phi(x)| = f(x), x \in \Omega, \quad \phi(x) = g(x), x \in \Gamma \subset \Omega, \quad (1)$$

where $f(x)$ is a positive function, corresponding to the slowness function.

There are mainly two classes of numerical methods for solving static Hamilton-Jacobi equations. The first class of numerical methods is based on reformulating the equations into suitable time-dependent problems. Osher (4) provides a natural link between static and time-dependent Hamilton-Jacobi equations by using the level-set idea and thus raising the problem one dimension higher. The zero-level set of the viscosity solution ψ of the time-dependent H-J equation

$$\psi_t + H(\psi_{x_1}, \dots, \psi_{x_d}, \phi, x) = 0 \quad (2)$$

at time t is the set of x such that $\phi(x) = t$ of (1), where the Hamiltonian H is homogeneous of degree one. Another approach to obtaining a “time” dependent H-J equation from the static H-J equation is using the so called paraxial formulation in which a preferred spatial direction is assumed in the characteristic propagation (1), (7). High order numerical schemes are well developed for the time dependent H-J equation (2) on structured and unstructured meshes (6; 2; 10).

The other class of numerical methods for static H-J equations is to treat the problem as a stationary boundary

value problem: discretize the problem into a system of nonlinear equations and design an efficient numerical algorithm to solve the system. Among such methods are the fast marching method and the fast sweeping method. In the fast marching method (9), the solution is updated by following the causality in a sequential way; i.e., the solution is updated pointwise in the order that the solution is strictly increasing (decreasing); hence two essential ingredients are needed in the algorithm: an upwind difference scheme and a heap-sort algorithm. The resulting complexity of the fast marching method is of order $O(N \log N)$ for N grid points, where the $\log N$ factor comes from the heap-sort algorithm. In the fast sweeping method (11), Gauss-Seidel iterations with alternating direction sweepings are incorporated into upwind finite differences. In contrast to the fast marching method, the fast sweeping method follows the causality along characteristics in a parallel way; i.e., all characteristics are divided into a finite number of groups according to their directions and each Gauss-Seidel iteration with a specific sweeping ordering covers a group of characteristics simultaneously. The fast sweeping method is optimal in the sense that a finite number of iterations is needed, so that the complexity of the algorithm is $O(N)$ for a total of N grid points; i.e., the number of iterations is independent of grid size. The algorithm is extremely simple to implement. The fast sweeping method is extended to solve more general Hamilton-Jacobi equations in (3).

However, the above cited fast sweeping methods are first-order schemes. In many applications, the numerical solutions from HJ equations are used to compute other quantities and thus their numerical derivatives are needed as well; for example, in geometrical optics the derivatives of traveltimes are used to compute amplitudes (8). Therefore, we develop high order fast sweeping methods for the static H-J equation (1). We adapt high order schemes for time dependent Hamilton-Jacobi equations in (6; 2; 10) to the static H-J equations in a novel way. First-order sweeping schemes are used as building blocks in our high order methods. The high order accuracy in our schemes results from the high order approximations for the partial derivatives because the monotone numerical Hamiltonians are Lipschitz continuous and consistent with the Hamiltonian H in the PDEs. In particular, we use the WENO approximations (2), since the weighted essentially non-oscillatory (WENO) approximations have uniform high order accuracy, and are more robust, and efficient than other schemes such as ENO schemes.

The algorithm is developed in Section 2. In Section 3, extensive numerical experiments are performed to demonstrate accuracy and fast convergence of the algorithms. High-order accuracy in smooth regions and good resolution of derivative singularities are observed. Concluding

Sweeping method for traveltimes

remarks are given in Section 4.

High order sweeping methods

We consider the two dimensional problems for simplicity. The extension to higher dimensions is straightforward.

We take $d = 2$ in (1):

$$\sqrt{\phi_x^2 + \phi_y^2} = f(x, y), (x, y) \in \Omega \quad (3)$$

$$\phi(x, y) = g(x, y), (x, y) \in \Gamma \subset \Omega. \quad (4)$$

Suppose that a rectangular mesh Γ_h covers the computational domain Ω . Let (i, j) denote a grid point in Γ_h , i.e., $\Gamma_h = \{(i, j), 1 \leq i \leq I, 1 \leq j \leq J\}$, where I and J are the indices of grid point in the x -direction and the y -direction, respectively. h_x and h_y denote uniform grid sizes at the x -direction and the y -direction respectively. To simplify the notation, we take $h_x = h_y = h$. $\phi_{i,j}$ denotes the numerical solution at the grid point (i, j) .

A first-order Godunov upwind difference scheme is used to discretize the PDE (3) as in (11):

$$\left[\left(\frac{\phi_{i,j} - \phi_{i,j}^{(x\min)}}{h} \right)^+ \right]^2 + \left[\left(\frac{\phi_{i,j} - \phi_{i,j}^{(y\min)}}{h} \right)^+ \right]^2 = f_{i,j}^2 \quad (5)$$

where $\phi_{i,j}^{(x\min)} = \min(\phi_{i-1,j}, \phi_{i+1,j}, \phi_{i,j}^{(y\min)}) = \min(\phi_{i,j-1}, \phi_{i,j+1})$ and

$$(x)^+ = \max(x, 0) \quad (6)$$

In order to construct a high-order scheme, we need to approximate the derivatives ϕ_x, ϕ_y with high-order accuracy. We choose to use the popular WENO approximations developed in (2). To illustrate the feasibility of the approach, we take the third order rather than fifth order WENO approximations; one certainly can replace the third order WENO with fifth order or even higher order WENO approximations. $(\phi_x)_{i,j}$ and $(\phi_y)_{i,j}$ denote approximations for ϕ_x and ϕ_y at grid point (i, j) , respectively. The approximation for ϕ_x at grid point (i, j) when the wind ‘‘blows’’ from the left to the right is

$$\begin{aligned} (\phi_x)_{i,j}^- &= (1 - w_-) \left(\frac{\phi_{i+1,j} - \phi_{i-1,j}}{2h} \right) \\ &\quad + w_- \left(\frac{3\phi_{i,j} - 4\phi_{i-1,j} + \phi_{i-2,j}}{2h} \right), \end{aligned} \quad (7)$$

where

$$w_- = \frac{1}{1 + 2r_-^2}, \quad r_- = \frac{\epsilon + (\phi_{i,j} - 2\phi_{i-1,j} + \phi_{i-2,j})^2}{\epsilon + (\phi_{i+1,j} - 2\phi_{i,j} + \phi_{i-1,j})^2}; \quad (8)$$

on the other hand, the approximation for ϕ_x at grid point (i, j) when the wind ‘‘blows’’ from the right to the left is

$$\begin{aligned} (\phi_x)_{i,j}^+ &= (1 - w_+) \left(\frac{\phi_{i+1,j} - \phi_{i-1,j}}{2h} \right) \\ &\quad + w_+ \left(\frac{-\phi_{i+2,j} + 4\phi_{i+1,j} - 3\phi_{i,j}}{2h} \right), \end{aligned} \quad (9)$$

where

$$w_+ = \frac{1}{1 + 2r_+^2}, \quad r_+ = \frac{\epsilon + (\phi_{i+2,j} - 2\phi_{i+1,j} + \phi_{i,j})^2}{\epsilon + (\phi_{i+1,j} - 2\phi_{i,j} + \phi_{i-1,j})^2}. \quad (10)$$

Similarly for $(\phi_y)_{i,j}^-$ and $(\phi_y)_{i,j}^+$.

Next we have to incorporate these high order approximation (7)-(10) for derivatives into monotone numerical Hamiltonians. In the case of eikonal equations, the numerical Hamiltonian under consideration is (5). In order to achieve this, we notice that the following identities hold:

$$(\phi_x)_{i,j}^- = \frac{\phi_{i,j} - [\phi_{i,j} - h \cdot (\phi_x)_{i,j}^-]}{h}, \quad (11)$$

$$(\phi_x)_{i,j}^+ = \frac{[\phi_{i,j} + h \cdot (\phi_x)_{i,j}^+] - \phi_{i,j}}{h}, \quad (12)$$

$$(\phi_y)_{i,j}^- = \frac{\phi_{i,j} - [\phi_{i,j} - h \cdot (\phi_y)_{i,j}^-]}{h}, \quad (13)$$

$$(\phi_y)_{i,j}^+ = \frac{[\phi_{i,j} + h \cdot (\phi_y)_{i,j}^+] - \phi_{i,j}}{h}. \quad (14)$$

According to the definitions of $(\phi_x)_{i,j}^-$ and $(\phi_x)_{i,j}^+$, $\phi_{i,j} - h \cdot (\phi_x)_{i,j}^-$ can be considered as an approximation to $\phi_{i-1,j}$ while $\phi_{i,j} + h \cdot (\phi_x)_{i,j}^+$ can be considered as an approximation to $\phi_{i+1,j}$. Similarly in (13) and (14), $\phi_{i,j} - h \cdot (\phi_y)_{i,j}^-$ and $\phi_{i,j} + h \cdot (\phi_y)_{i,j}^+$ can be considered as approximations to $\phi_{i,j-1}$ and $\phi_{i,j+1}$, respectively. Replacing $\phi_{i-1,j}, \phi_{i+1,j}, \phi_{i,j-1}, \phi_{i,j+1}$ with these approximations in equation (5), we have the following high order schemes,

$$\left[\left(\frac{\phi_{i,j}^{new} - \phi_{i,j}^{(x\min)}}{h} \right)^+ \right]^2 + \left[\left(\frac{\phi_{i,j}^{new} - \phi_{i,j}^{(y\min)}}{h} \right)^+ \right]^2 = f_{i,j}^2 \quad (15)$$

where

$$\phi_{i,j}^{(x\min)} = \min(\phi_{i,j}^{old} - h \cdot (\phi_x)_{i,j}^-, \phi_{i,j}^{old} + h \cdot (\phi_x)_{i,j}^+), \quad (16)$$

$$\phi_{i,j}^{(y\min)} = \min(\phi_{i,j}^{old} - h \cdot (\phi_y)_{i,j}^-, \phi_{i,j}^{old} + h \cdot (\phi_y)_{i,j}^+). \quad (17)$$

$\phi_{i,j}^{new}$ denotes the to-be-updated numerical solution for ϕ at the grid point (i, j) , and $\phi_{i,j}^{old}$ denotes the current old value for ϕ at the grid point (i, j) . When WENO approximations for derivatives $(\phi_x)_{i,j}^-, (\phi_x)_{i,j}^+, (\phi_y)_{i,j}^-, (\phi_y)_{i,j}^+$ in (16) are computed according to formulae (7-10), we always use the newest available values for ϕ in the interpolation stencils according to the philosophy of Gauss-Seidel type iterations. Of course, since we have not updated $\phi_{i,j}$ yet, $\phi_{i,j}^{old}$ is used in (7-10). The solution for the equation (15) is $\phi_{i,j}^{new} = \min(\phi_{i,j}^{(x\min)}, \phi_{i,j}^{(y\min)}) + f_{i,j}h$ if $|\phi_{i,j}^{(x\min)} - \phi_{i,j}^{(y\min)}| \geq f_{i,j}h$; otherwise, $\phi_{i,j}^{new} = \frac{\phi_{i,j}^{(x\min)} + \phi_{i,j}^{(y\min)} + \sqrt{2f_{i,j}^2 h^2 - (\phi_{i,j}^{(x\min)} - \phi_{i,j}^{(y\min)})^2}}{2}$.

The first order scheme (5) is monotone and hence the convergence is guaranteed (see (11)). There is no such

Sweeping method for traveltimes

monotonicity for the high order scheme (15)-(16). A reliable initial guess is needed for the convergence of the Gauss-Seidel iterations. In other words, to achieve fast convergence we wish to have $\phi_{i,j} - h \cdot (\phi_x)_{i,j}^-$, $\phi_{i,j} + h \cdot (\phi_x)_{i,j}^+$, $\phi_{i,j} - h \cdot (\phi_y)_{i,j}^-$, $\phi_{i,j} + h \cdot (\phi_y)_{i,j}^+$ as good approximations of $\phi_{i-1,j}$, $\phi_{i+1,j}$, $\phi_{i,j-1}$, $\phi_{i,j+1}$, respectively, so that the causality of the true solution is approximately right. In all our implementations we use the first order scheme, which is robust and efficient, to provide a good initial guess.

We summarize the high order fast sweeping method for the eikonal equation (3) as following:

1. Initialization: according to the boundary condition $\phi(x, y) = g(x, y)$, $(x, y) \in \Gamma$, assign exact values or interpolated values at grid points whose distances to Γ are less than $(n - 1)h$, where n is the number of grid points in the small stencil in WENO approximations. For example, $n = 3$ for the third order WENO approximations. These values are fixed during iterations. The solution from the first-order fast sweeping method is used as the initial guess at all other grid points.
2. Iterations: solve the discretized nonlinear system (15) by Gauss-Seidel iterations with four alternating direction sweepings:

$$\begin{aligned} (1) & i = 1 : I, j = 1 : J; \\ (2) & i = I : 1, j = 1 : J; \\ (3) & i = I : 1, j = J : 1; \\ (4) & i = 1 : I, j = J : 1, \end{aligned}$$

Equations (7)-(10) and equations (16)-(17) are used to solve (15). High order extrapolations are used for the ghost points when calculating the high order WENO approximations of derivatives (7)-(10) for grid points on the boundary of the computational domain. For example, we use fourth order extrapolation for our third order fast sweeping method.

3. Convergence: if

$$\|\phi^{new} - \phi^{old}\|_{L^1} \leq \delta,$$

where δ is a given convergence threshold value, the algorithm converges and stops.

Numerical Examples

We apply the high order fast sweeping methods to some typical two dimensional problems. Third order WENO approximations are used. In all the examples, the threshold value at which iteration stops is taken to be $\delta = 10^{-11}$.

Table 1: Γ is a point. Initial Values are given in the box with length 0.3 which includes the source point.

mesh	L^1 error	order	L^∞ error	order	iter
40×40	1.56E-4	-	2.88E-4	-	30
80×80	2.80E-6	5.80	5.60E-6	5.69	28
160×160	6.64E-7	2.08	1.28E-6	2.12	32
320×320	9.70E-8	2.78	1.83E-7	2.81	44
640×640	1.23E-8	2.98	2.32E-8	2.98	68

Example 1. Eikonal equation (3) with $f(x, y) = 1$. The computational domain is $\Omega = [-1, 1] \times [-1, 1]$, and Γ is a source point with coordinates $(0, 0)$. So the exact solution is the distance function to the source point Γ . The solution is singular at the source point. Since all characteristics emit from this source point like rarefaction waves in hyperbolic conservation law, errors made at the source point will propagate out and pollute the solution in the whole computational domain. We illustrate this delicate point with different initializations near the source point.

First we assign the exact values to a small region which encloses the source point, say, a small box with length 0.3. This box size is fixed during the mesh refinement study. Accuracy and errors are reported in Table 1. We can see that the perfect third order accuracy is obtained.

Next we initialize the solution near the source point by fixing the number of grid points during the mesh refinement study. Thus the box which encloses the source point is taken to have length $2h$, where h is the mesh size. Accuracy and errors are reported in Table 2. We can see that the third order accuracy can not be obtained any more. If Γ has source points or corners from which the characteristics propagate and form rarefaction wave regions, the error incurred at the singular point will propagate to affect the solution in the smooth region, hence leading to the loss of accuracy. Of course, if a fixed small domain is used to wrap the singular corner point, i.e., exact values are assigned to the small region, the high order accuracy can be achieved. The most efficient way to recover such loss of accuracy is to use adaptive meshes with good a posteriori estimates near singularities; see (8) for such an adaptive method in the paraxial formulation.

In Table 3, we also list the errors and accuracy for first order fast sweeping method (5). In comparison with the high order results in Table 1 and 2, we can see that the high order schemes do achieve much smaller errors than a low order method does on the same grids.

Example 2. Eikonal equation (3) with $f(x, y) = 1$. The computational domain $\Omega = [-2, 2] \times [-2, 2]$, and Γ is a sector of three quarters of a circle not shown here. So the exact solution is the distance function to the sector Γ . Singularities at three corners in Γ give rise to different scenarios in different regions, which include both shocks and rarefaction waves. During the mesh refinement study, we fix the number of grid points when we initialize the domain. Third order accuracy is obtained for smooth

Sweeping method for traveltimes

Table 2: Γ is a point. Initial Values are given in the box with length $2h$ which includes the source point.

mesh	L^1 err.	order	L^∞ err.	order	iter
40×40	1.35E-3	–	2.52E-3	–	59
80×80	6.32E-4	1.10	1.17E-3	1.11	41
160×160	2.37E-4	1.41	4.69E-4	1.31	43
320×320	5.02E-5	2.24	1.20E-4	1.97	59

Table 3: Γ is a point. Initial Values are given in the box with length $2h$ which includes the source point. First order scheme.

mesh	L^1 err.	order	L^∞ err.	order	iter
40×40	1.88E-2	–	3.79E-2	–	1
80×80	1.30E-2	0.54	2.46E-2	0.63	1
160×160	8.34E-3	0.64	1.52E-2	0.70	1
320×320	5.11E-3	0.71	9.07E-3	0.74	1

solution regions. Moreover, we still obtain second-order accuracy in the whole computational domain; see Table 4. The accuracy in rarefaction wave region is consistent with the results in Example 1. We also plot the 3D pictures of the numerical solution with mesh 80×80 in Fig. 1; we can observe the sharp shock transition in the figure.

Concluding remarks

We have developed high order fast sweeping methods for static Hamilton-Jacobi equations on rectangular meshes. A general procedure is given to incorporate the high order approximations into monotone numerical Hamiltonians so that the first order sweeping schemes can be extended to high order schemes. Numerical examples demonstrate that the high order methods yield the high order accuracy in the smooth region of the solution, high resolution for the singularities of derivatives, and fast convergence to viscosity solutions of the Hamilton-Jacobi equations.

References

S.Gray and W.May, *Kirchhoff migration using eikonal equation travel-times*, Geophysics, 59 (5) (1994), 810-

Table 4: Accuracy in different regions.

mesh	smooth region		whole region		iter
	L^1 error	order	L^1 err.	order	
80×80	1.03E-5	–	1.70E-4	–	38
160×160	1.32E-6	2.96	6.09E-5	1.48	26
320×320	2.89E-7	2.19	1.72E-5	1.82	34
640×640	4.03E-8	2.84	4.13E-6	2.06	53

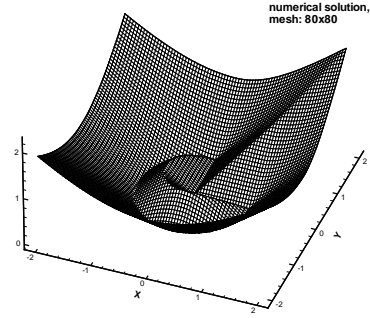


Fig. 1: Computed distance to Γ , where Γ is a sector

817.

G.-S. Jiang and D. Peng, *Weighted ENO Schemes for Hamilton-Jacobi equations*, SIAM Journal on Scientific Computing, v21 (2000), pp.2126–2143.

C.Y. Kao, S. Osher and J. Qian, *Lax-Friedrichs sweeping scheme for static Hamilton-Jacobi equations*, Journal of Computational Physics, to appear.

S. Osher, *A level set formulation for the solution of the Dirichlet problem for Hamilton-Jacobi equations*, SIAM J. Math. Anal. 24 (5) (1993), 1145-1152.

S. Osher and J. Sethian, *Fronts propagating with curvature dependent speed: algorithms based on Hamilton-Jacobi formulations*, Journal of Computational Physics, v79 (1988), pp.12–49.

S. Osher and C.-W. Shu, *High-order essentially nonoscillatory schemes for Hamilton-Jacobi equations*, SIAM Journal on Numerical Analysis, v28 (1991), pp.907–922.

J.Qian and W.W.Symes, *Finite-difference quasi-P traveltimes for anisotropic media*, Geophysics, 67 (2002) 147-155.

J.Qian and W.W.Symes, *An adaptive finite-difference method for traveltime and amplitude*, Geophysics, 67 (2002) 166-176.

J.A. Sethian, *A fast marching level set method for monotonically advancing fronts*, Proc. Nat. Acad. Sci., 1996.

Y.-T. Zhang and C.-W. Shu, *High order WENO schemes for Hamilton-Jacobi equations on triangular meshes*, SIAM Journal on Scientific Computing, 24 (2003), 1005-1030.

H.-K. Zhao, *A fast sweeping method for Eikonal equations*, Math. Comp. (2003), to appear.